MEDWIN PUBLISHERS
Committed to Create Value for Researchers

Nanomedicine & Nanotechnology Open Access
ISSN: 2574-187X

Characterization of Chitosan-Titanium Oxide-Silver Nanocomposite Synthesized by Pulsed Laser Ablation in Liquid

Zaid Hassoun TA, Al-Nafiey A* and Abd JA

Department of Laser Physics, University of Babylon, Iraq

***Corresponding author:** Amer Al-Nafiey, Department of Laser Physics, College of Science for Women, University of Babylon, Iraq, Email: amer76z@yahoo.com

Research Article
Volume 8 Issue 3
Received Date: August 24, 2023
Published Date: September 25, 2023
DOI: 10.23880/nnoa-16000254

Abstract

Chitosan-titanium oxide-silver CS-TiO_2-Ag nanocomposite was successfully synthesized using pulsed laser ablation in liquid with a frequency of 1 Hz and energy of 500 mJ, and the number of pulses of titanium and silver plates was 1000 and 500, respectively. The resulting nanocomposite was characterized using various techniques, including FTIR, UV-vis, X-ray diffraction, and SEM. The FTIR analysis showed that the chemical bonds of chitosan were superimposed with silver and titanium oxide. UV-vis spectrum showed that the absorbance peaks for CS-Ag and CS-TiO_2 at 399.9 nm and 242 nm, respectively, and the calculating energy gaps of the CS-TiO_2,CS-Ag and CS-TiO_2-Ag nanocomposites are found to be (4.18 , 2.82 and 2.74) eV, respectively. The SEM images for CS-TiO_2-Ag showed that the shape as semi-spherical, and the average grain size of the nanoparticles is 95 nm. Moreover, the X-ray diffraction analysis revealed that TiO2 and Ag were polycrystalline and that the average crystallite sizes for CS-Ag, CS-TiO_2, and CS-TiO_2-Ag were 5.96, 5.96, and 5.95 nm, respectively.
This study demonstrated that pulsed laser ablation in liquid is an easy and safe method for synthesizing CS-TiO_2-Ag nanocomposites that can be used in various applications. The characterization techniques used in this study provided valuable insights into the properties and structures of the synthesized nanocomposite material.

Keywords: Chitosan; Titanium Oxide; Silver; Pulsed Laser Ablation of Liquid; Optical Properties; X-Ray Diffraction; Scanning Electron Microscope (SEM)

Abbreviations: SEM: Scanning Electron Microscope; EDX: Energy Dispersive X-ray Spectroscopy.

Introduction

Nanometals and metal oxide including gold, zinc, copper, silver, titanium, zinc oxide, silver oxide, and titanium oxide have attracted great attention recently in medical, chemical, and optoelectronics applications due to their chemical and physical properties [1]. Therefore, titanium oxide (TiO_2) is a naturally occurring mineral that is widely used in various industrial and commercial applications due to its unique properties. Meanwhile, Silver (Ag) is chemical element with a highly conductivity and is often using in electrical and electronic, and other application. Silver has a high level of ductility and malleability, which makes it easy to shape into different forms [2]. On the other hand, polymers have been used with nanomaterials to enhance one another's properties [3] such as polyvinyl alcohol [4], polystyrene [5] and Chitosan (CS) [6].

In general, nanomaterials (NMs) can be synthesized using two methods: chemical methods such as Sol-Gel method [7], electrochemical synthesis [8], and physical methods such as

Gas Phase Condensation [9], Solvent Evaporation [10], Ball Milling [11], and laser ablation [12].

In recent years, many reports have synthesized the nanocomposites CS-TiO_2 by the laser ablation method [13,14], CS-TiO_2 by a homogenization approach and by chemical reduction [15,16], as well as CS-Ag by the pulse laser ablation [17] and by Electrodeposition [18], In addition, the compound CS-Ag-TiO_2 was synthesized by the chemical method [19].

As known, pulsed laser ablation has been utilized to prepare nanomaterials by focusing the laser beam on a solid target immersed in a liquid solution, where the target absorbs the heat from the laser, generates plasma, and then nanoparticles are obtained [20]. This method is safer and more environmentally friendly than other methods. It allows for the control of the laser parameters used, including laser energy, wavelength, pulsed number, repetition rate, and frequency, to obtain nanoparticles of an appropriate size [21].

In this research, the CS-TiO_2-Ag nanocomposites were synthesized by pulsed laser ablation in liquid, and the properties of the nanocomposite were studied.

Material

High purity chitosan powder with a molecular weight of 1,500,000 g/mol was purchased from Life Sciences (GP5053) 0.5 (g). Silver and titanium plates (purity 99.8%) were also purchased from commercial market as target metal substrates.

Experimental

The chitosan was dissolved in a mixture of water (670 ml) and acetic acid (70 ml). Silver nanoparticles were prepared by pulsed laser ablation in liquids; a silver plate was placed in a previously prepared chitosan solution. A Nd:YAG laser with a wavelength of 1064 nm was used, with an energy of 500 mJ, a pulse number of 500 pulses, and a frequency of 1 Hz. Similarly, titanium nanoparticles were prepared using the same ablation method with same parameters, but with a higher number of pulses (1000 pulses). Thus, CS-TiO_2-Ag was synthesized.

The CS-Ag and CS-TiO_2 nanocomposites were prepared separately in the same chitosan solution, and the same laser parameters mentioned above were used for each sample CS, CS-Ag, CS-TiO_2, and CS-TiO_2-Ag. These samples were deposited on aluminum pieces for EDX and SEM analysis. In addition, the same samples were placed on a glass slide for XRD analysis. The liquid was used to perform the analyses (FTIR, and UV-Vis).

Results and Discussion

UV-Vis septum shows that the peak of CS-Ag is at 400 nm, and for CS-TiO2, the peak is at 242 nm. For CS-TiO_2-Ag, the peak position has no change, but the intensity of absorption had been changed due to the increasing in the concentration of nanoparticles in the solution [22,23], where the increment in the intensity of (CS-TiO_2) and the decreasing of (CS-Ag) intensity of the composite (CS-TiO_2-Ag) due to the presence of core-shell, which means that the silver is surrounded by titanium [24] as shown in (Figure 1).

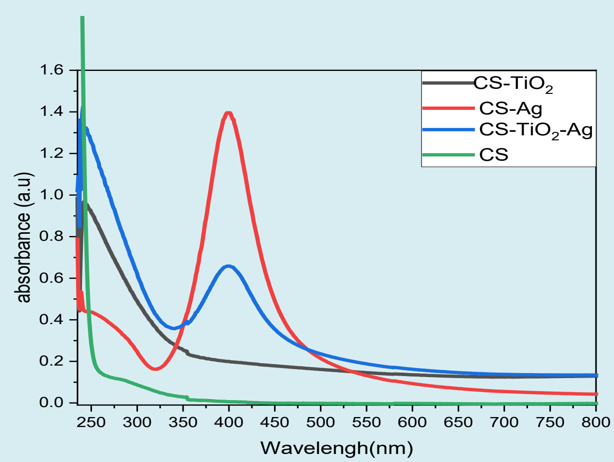

Figure 1: UV–vis spectra of the CS –Ag, CS-TiO_2, CS-TiO_2-Ag, CS.

Beer-Lambert law has been used to calculate the absorption coefficient, equation (1) [25];

$$\alpha = 2.303A/t \quad (1)$$

Where α: absorption coefficient

A: absorbance

t: thickness

As shown in (Figure 2), the high absorption coefficient at 224 nm and 399.9 nm represented the TiO_2 and Ag respectively.

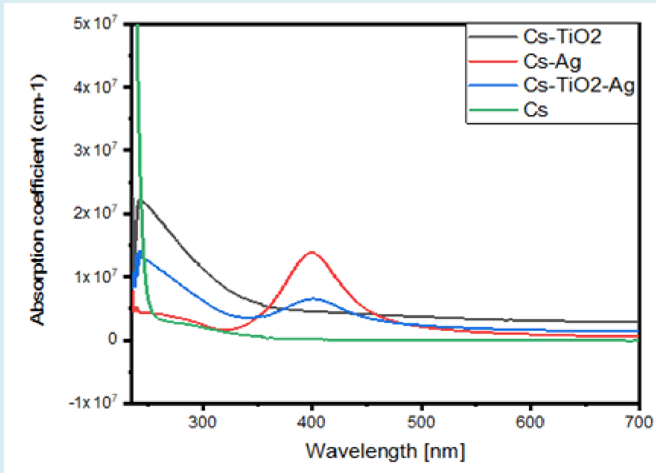

Figure 2: The absorption coefficient for CS, CS-Ag, CS-TiO_2, and CS-TiO_2-Ag.

The Tauc plot method is based on the assumption that the energy-dependent absorption coefficient α can be expressed by equation (2) [26]:

$$(\alpha \cdot h\nu)^{1/\gamma} = B(h\nu - E_g) \quad (2)$$

where h is the Planck constant, ν is the photon's frequency, Eg is the band gap energy, and B is a constant.

So, the energy gaps of the CS-TiO_2, CS-Ag and CS-TiO_2-Ag are (4.18, 2.82 and 2.74) eV, respectively as shown in Figure 3. Titanium oxide is a semi-conducting oxide, and when it is doped with chitosan polymer, it creates secondary levels in the energy gap between the valence band and the conductive band, as is the case with silver nanoparticles [27,28].

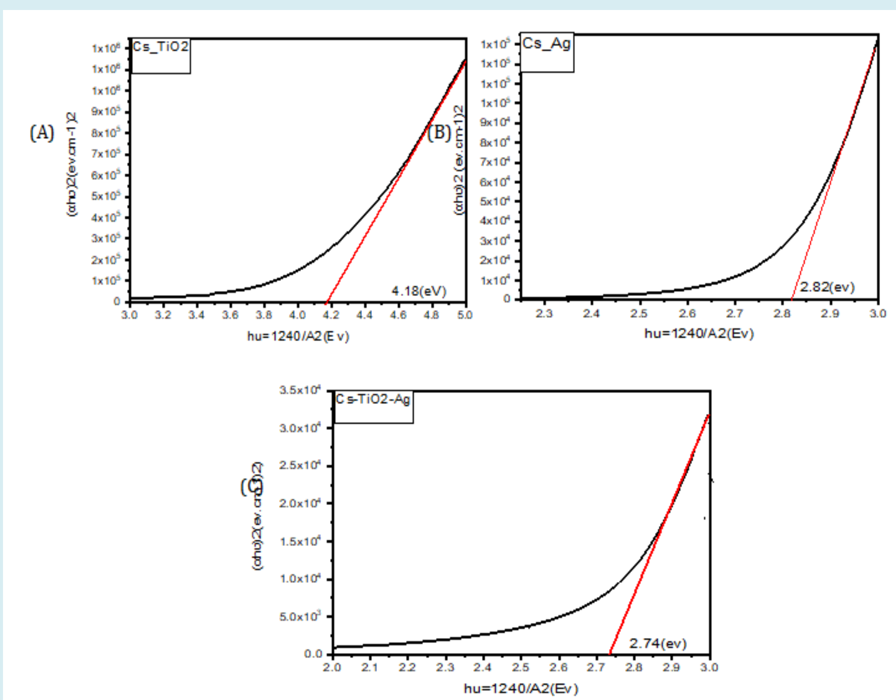

Figure 3: The Energy Band Gap for: A (CS-TiO_2), B (CS-Ag), C (CS-TiO_2-Ag).

As is known, infrared spectroscopy is a powerful tool for analyzing the functional groups present in molecules. In general, the position and shape of peaks in the infrared spectrum can be used to identify specific functional groups within the molecule [29]. Figure 4 shows the chemical bonds (C-H, C-N, O-H, C-O, C-O-C, COO, C=H, C=C) to the chitosan polymer, which are present in all samples, and in the sample CS-Ag, the bond of silver with the polymer is followed by bonds (Ag-NH_2, Ag-O). In the sample, CS-TiO_2 bonds also appeared, indicating the presence of titanium in the polymer (Ti-O-Ti) and the sample CS-TiO_2-Ag revealed links indicating the presence of both silver and titanium (Ag-O, Ti-O, Ti-C). These results indicate that the TiO_2 and Ag nanoparticles are present in the matrix of the CS polymer [30-34]

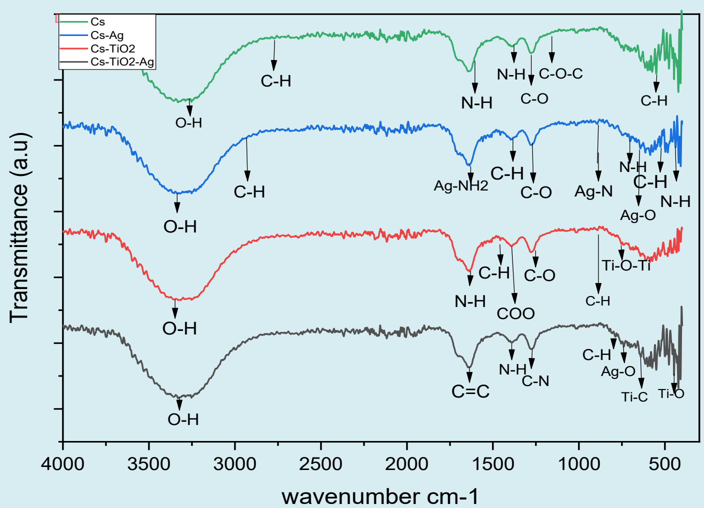

Figure 4: The FTIR for: CS-Ag, CS-TiO_2, CS-TiO_2-Ag, CS.

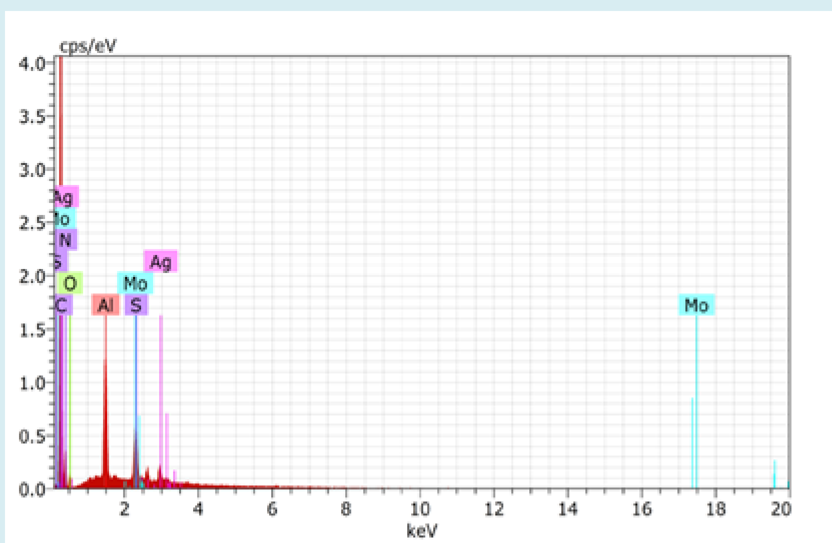

Figure 5: The EDX for (CS-Ag).

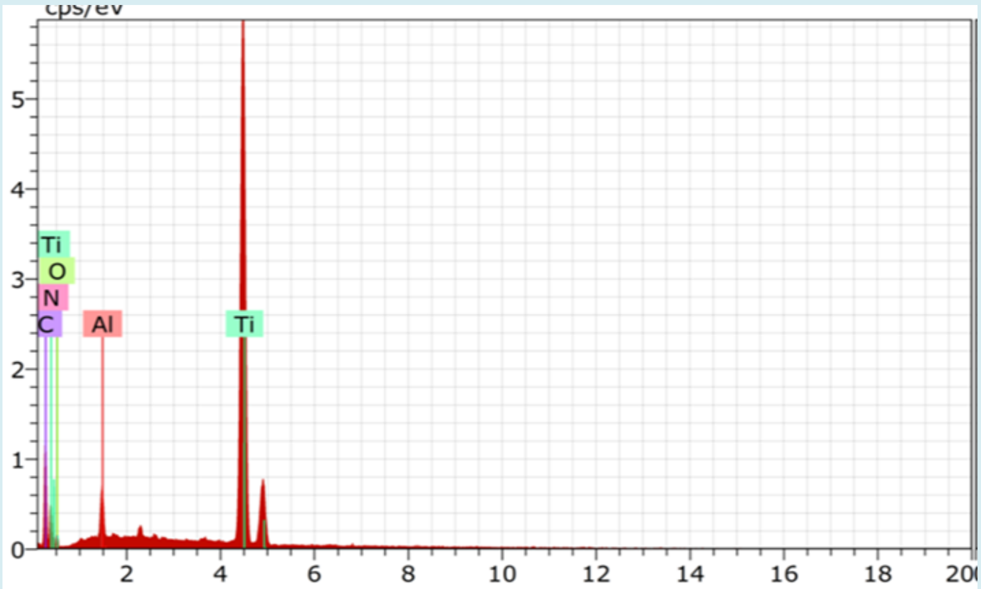

Figure 6: the EDX for (CS-TiO2).

C [wt.%]	Materials
67.78	Ag
14.76	N
10.22	C
4.37	O
2.1	Al
0.77	Mo

Table 1: The EDX for (CS-Ag).

C Error [wt.%]	Materials
23.08	Ti
36.25	C
19.66	N
19	O
2	Al

Table 2: The EDX for (CS-TiO_2).

In Figures 5 & 6, as well as Tables 1 & 2, Energy Dispersive X-ray Spectroscopy (EDX) analysis revealed the presence of various elements. Elements such as carbon (C), nitrogen (N), and oxygen (O) were attributed to chitosan, consistent with findings as reports [35,36]. Furthermore, the appearance of silver (Ag) and titanium (Ti) indicates the presence of silver and titanium nanoparticles. The detection of aluminum (Al) and molybdenum (Mo) could potentially stem from contamination originating from the sample holder.

Moreover, the X-ray diffraction technique was used to study the crystal structures of CS-TiO_2, CS-Ag and CS-TiO_2-Ag. For CS-TiO_2, the diffraction spectrum in (Figure 7B) shows the peaks at (2θ = 29.701, 37.42), directions (101, 401), and intensity (110), (110), respectively. These angles coincided with the International Card for Titanium Oxide (46-1238). While (Figure 7C) shows the X-ray diffraction spectrum of CS-Ag, which showed diffraction peaks at (2θ= 29.54, 32.03, 35.32, 37.27) corresponding to a previous study [37] and the International Silver Card (41-1402) and in the direction of (331), (131), (100), (101) with intensity (100, 100, 20, 50) respectively.

Additionally, for the CS-TiO_2-Ag, its diffraction spectrum was as shown in (Figure 7D), at (2θ = 29.655, 32.172, 37.328), directions (204), (404), (205) and intensity (150, 800, 100) respectively, its combatable with the international card (32.1028).

The angles were repeated in the CS-Ag, and CS-TiO_2 with the angles of the CS-TiO_2-Ag, but the angles (29, 32, and 37) were different in intensity as shown above.

Peaks appeared for CS-Ag more than peaks for CS-TiO_2, although the number of pulses used in the ablation of titanium is more than the number of pulses used in silver, because of the high bonding energy of titanium, where it needs a higher number of pulses to get rid of the bonds between its atoms [38-40].

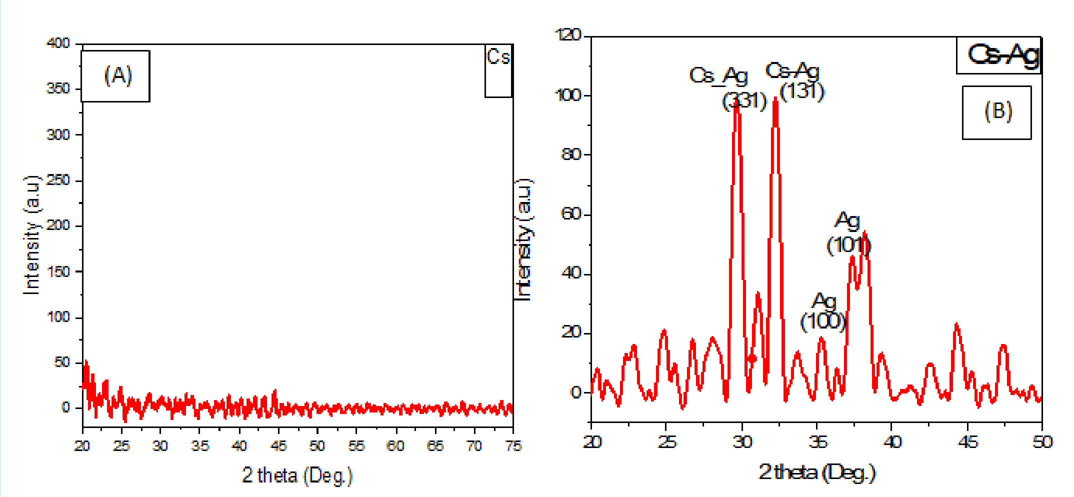

Figure 7: XRD for A (CS), B(CS-TiO_2), C (CS-Ag) and D (CS-TiO_2-Ag**).**

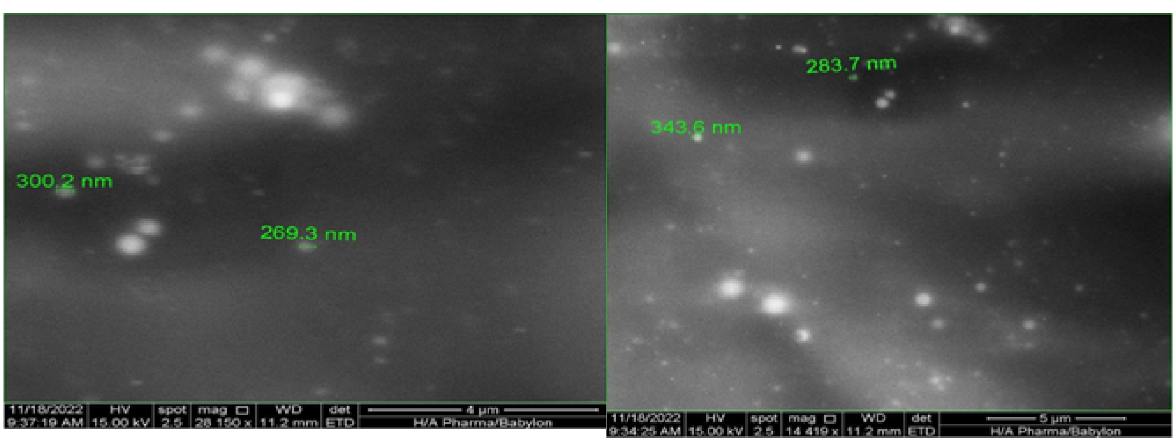

Figure 8: The SEM CS-TiO_2-Ag.

In the scanning electron microscope (SEM) images as in (Figure 8), sheet of chitosan formed with silver and titanium dioxide appeared in the form of white dots, and the grain size was different and the average grain size was 95 nm. Taking into account that the small sizes could not be calculated by the Image program.

Conclusions

In this study, we have successfully prepared nanocomposites CS-TiO_2-Ag, CS-Ag, and CS-TiO_2 using the innovative technique of pulsed laser ablation in liquid. The absorbance spectra analysis yielded valuable insights, revealing distinct peaks at 242 nm and 400 nm, corresponding to titanium dioxide and silver, respectively. Moreover, the calculated bandgap energies for CS-TiO_2, CS-Ag, and CS-TiO_2-Ag were found to be 4.18 eV, 2.82 eV, and 2.74 eV, respectively.

Our investigation into the crystalline structures through X-ray diffraction analysis unveiled commendable crystalline qualities in all compounds. Remarkably, the average crystalline sizes for CS-Ag, CS-TiO_2, and CS-TiO_2-Ag were determined to be 5.96 nm, 5.96 nm, and 5.95 nm, respectively, indicating fine crystallinity in the materials.

Chemical interactions among these compounds were systematically confirmed via FTIR analysis, demonstrating the successful formation of the nanocomposites. Visual examination of the SEM images showcased an average grain size of approximately 95 nm for the Ag and TiO_2 materials, effectively adhering to the chitosan substrate.

References

1. Bovykin DV, Friedrich JM, Walsh FC (2006) Protonated titanates and TiO_2 nanostructured materials: synthesis, properties, and applications. Advanced materials 18(21): 2807-2824.
2. Hilliard HE (2003) Silver recycling in the United States in 2000. US Geological Survey.
3. Peggiani S, Facibeni A, Milani A, Castiglioni C, Russo V, et al. (2020) In situ synthesis of polyenes in a polymer matrix via pulsed laser ablation in a liquid. Materials Advances 1(8): 2729-2736.
4. Mostafa AM, Menazea AA (2020) Polyvinyl Alcohol/ Silver nanoparticles film prepared via pulsed laser ablation: An eco-friendly nano-catalyst for 4-nitrophenol degradation. Journal of Molecular Structure 1212: 128125.
5. Jiao K, Yang B, Wang H, Xu W, Zhang C, et al. (2022) The individual and combined effects of polystyrene and silver nanoparticles on nitrogen transformation and bacterial communities in an agricultural soil. Science of the Total Environment 820: 153358.
6. Ali H, Ismail AM, Menazea AA (2022) Multifunctional Ag/ ZnO/chitosan ternary bio-nanocomposites synthesized via laser ablation with enhanced optical, antibacterial, and catalytic characteristics. Journal of Water Process Engineering 49: 102940.
7. Brinker CJ, Scherer GW (2013) Sol-gel science: the physics and chemistry of sol-gel processing. Academic press.
8. Bard AJ, Faulkner LR, White HS (2022) Electrochemical methods: fundamentals and applications. In: 3rd (Edn.), John Wiley & Sons.
9. Huttel Y (2017) Gas-phase synthesis of nanoparticles. John Wiley & Sons.
10. McGinity JW, O Donnell PB (1997) Preparation of microspheres by the solvent evaporation technique. Advanced drug delivery reviews 28(1): 25-42.
11. Chen D, Li L, Wang JH (2013) One-step synthesis of zinc ferrite nanoparticles by ultrasonic wave-assisted ball milling technology. CeramiCS International 39(4): 4669-4672.
12. Naser H, Alghoul MA, Hossain MK, Asim N, Abdullah MF, et al. (2019) The role of laser ablation technique parameters in synthesis of nanoparticles from different target types. Journal of Nanoparticle Research 21: 1-28.
13. Li B, Zhang Y, Yang Y, Qiu W, Wang X, et al. (2016) Synthesis, characterization, and antibacterial activity of chitosan/TiO_2 nanocomposite against Xanthomonas oryzae pv. oryzae. Carbohydrate Polymers 152: 825-831.
14. Tatarinov D, Sokolnikova S, Myslitskaya N (2021) Applying of chitosan-TiO_2 nanocomposites for photocatalytic degradation of anthracene and pyrene. Journal of Biomedical Photonics & Engineering 7(1): 010301.
15. Tatarinov DA, Sokolnikova SR, Myslitskaya NA (2021) A study of the photocatalytic properties of chitosan-TiO_2 composites for pyrene decomposition. Journal Scientific and Technical Of Information Technologies, Mechanics and Optics 135(5): 670.
16. Spoială A, Ilie CI, Dolete G, Croitoru AM, Surdu VA, et al. (2022) Preparation and characterization of chitosan/ TiO_2 composite membranes as adsorbent materials for water purification. Membranes 12(8): 804.
17. Razzaq AA, Al Nafiey A, Al Marzoqy A (2022) Decorated

chitosan with silver-zinc nanoparticles by pulse laser ablation. Results in Optics 9: 100282.

18. Wang Y, Guo X, Pan R, Han D, Chen T, et al. (2015) Electrodeposition of chitosan/gelatin/nanosilver: A new method for constructing biopolymer/nanoparticle composite films with conductivity and antibacterial activity. Materials Science and Engineering: C 53: 222-228.

19. Jbeli A, Hamden Z, Bouattour S, Ferraria AM, Conceição DS, et al. (2018) Chitosan-Ag-TiO_2 films: an effective photocatalyst under visible light. Carbohydrate polymers 199: 31-40.

20. Zhang J, Chaker M, Ma D (2017) Pulsed laser ablation based synthesis of colloidal metal nanoparticles for catalytic applications. Journal of colloid and interface science 489: 138-149.

21. Yu J, Nan J, Zeng H (2017) Size control of nanoparticles by multiple-pulse laser ablation. Applied Surface Science 402: 330-335.

22. BinSabt M, Sagar V, Singh J, Rawat M, Shaban M (2022) Green synthesis of CS-TiO_2 NPs for efficient photocatalytic degradation of methylene blue dye. Polymers 14(13): 2677.

23. Tajdidzadeh M, Azmi BZ, Yunus WMM, Talib ZA, Sadrolhosseini AR, et al. (2014) Synthesis of silver nanoparticles dispersed in various aqueous media using laser ablation. The Scientific World Journal 2014.

24. Pastoriza Santos I, Koktysh DS, Mamedov AA, Giersig M, Kotov NA, et al. (2000) One-pot synthesis of Ag@ TiO_2 core− shell nanoparticles and their layer-by-layer assembly. Langmuir 16(6): 2731-2735.

25. Skoog DA, West DM, Holler FJ, Crouch SR (2013) Fundamentals of analytical chemistry. Cengage learning.

26. Colinge JP, Colinge CA (2002) Physics of semiconductor devices. Springer Science & Business Media.

27. Nabi G, Ain QU, Tahir MB, Nadeem Riaz K, Iqbal T, et al. (2022) Green synthesis of TiO_2 nanoparticles using lemon peel extract: their optical and photocatalytic properties. International Journal of Environmental Analytical Chemistry 102(2): 434-444.

28. Dolgonos A, Mason TO, Poeppelmeier KR (2016) Direct optical band gap measurement in polycrystalline semiconductors: A critical look at the Tauc method. Journal of solid state chemistry 240: 43-48.

29. Moradpoor H, Safaei M, Golshah A, Mozaffari HR, Sharifi R, et al. (2021) Green synthesis and antifungal effect of titanium dioxide nanoparticles on oral *Candida albicans* pathogen. Inorganic Chemistry Communications 130: 108748.

30. Su C, Berekute AK, Yu KP (2022) Chitosan@ TiO_2 composites for the adsorption of copper (II) and antibacterial applications. Sustainable Environment Research 32(1): 1-15.

31. Govindan S, Nivethaa EAK, Saravanan R, Narayanan V, Stephen A (2012) Synthesis and characterization of chitosan–silver nanocomposite. Applied Nanoscience 2: 299-303.

32. Rajeshkumar S (2021) Citrus lemon juice mediated preparation of AgNPs/chitosan-based bionanocomposites and its antimicrobial and antioxidant activity. Journal of Nanomaterials 2021: 1-10.

33. Haldorai Y, Shim JJ (2014) Novel chitosan-TiO_2 nanohybrid: Preparation, characterization, antibacterial, and photocatalytic properties. Polymer Composites 35(2): 327-333.

34. Dole MN, Patel PA, Sawant SD, Shedpure PS (2011) Advance applications of Fourier transform infrared spectroscopy. Int J Pharm Sci Rev Res 7(2): 159-166.

35. Foot CJ (2004) Atomic physics. OUP Oxford, 7: 344.

36. Samuels RJ (1981) Solid state characterization of the structure of chitosan films. Journal of polymer science: polymer physics edition 19(7): 1081-1105.

37. Kumar Krishnan S, Prokhorov E, Hernández Iturriaga M, Mota Morales JD, Vázquez Lepe M, et al. (2015) Chitosan/silver nanocomposites: Synergistic antibacterial action of silver nanoparticles and silver ions. European Polymer Journal 67: 242-251.

38. Gong S, Liu BG (2012) Electronic structures and optical properties of TiO_2: Improved density-functional-theory investigation. Chinese PhysiCS B 21(5): 057104.

39. Jian Zhi Z, Guang Tao W, Yong Cheng L (2008) Mechanical properties and electronic structures of cotunnite TiO_2. Chinese PhysiCS Letters 25(12): 4356.

40. Bhosale J, Ramdas AK, Burger A, Muñoz A, Romero AH, et al. (2012) Temperature dependence of band gaps in semiconductors: Electron-phonon interaction. Physical Review B 86(19): 195208.